

Structure and defects of detonation synthesis nanodiamond

K. Iakoubovskii ^{a,*}, M.V. Baidakova ^b, B.H. Wouters ^c, A. Stesmans ^a,
G.J. Adriaenssens ^a, A.Ya. Vul' ^b, P.J. Grobet ^c

^a Semiconductors Physics Laboratory, K.U. Leuven, Celestijnenlaan 200 D, B-3001 Heverlee, Belgium

^b Ioffe Physico-Technical Institute, Polytechnicheskaya 26, St. Petersburg 194021, Russia

^c Center for Surface Chemistry and Catalysis, K.U. Leuven, K. Mercierlaan 92, B-3001 Heverlee, Belgium

Abstract

Characterization of the structure and defects in detonation synthesis, ultradisperse diamond (UDD) is reported. X-ray and proton nuclear magnetic resonance results on UDD powders are interpreted in terms of the different structure of the shell of UDD particles, produced under different conditions. In spite of the comparable contents of carbon and nitrogen atoms in the precursor, no (<10 ppb) paramagnetic nitrogen was detected in the UDD grains. © 2000 Elsevier Science S.A. All rights reserved.

Keywords: Defect; IR; Nitrogen; sp² bonding

1. Introduction

The synthesis and investigation of nanomaterials are fascinating subjects in solid-state physics. The effect of the surface on the bulk properties becomes important when the particle size approaches the nanometer scale and this has stimulated both the scientific and technological interest of nanomaterials. The properties of nanoparticles of some metals and semiconductors have been well investigated and reviewed (e.g. see Ref. [1]); however, owing to difficulties in its synthesis, studies of the properties of nanodiamond powder are still rare. Nowadays, nanodiamond is generally produced from carbon contained in explosives by their detonation. Surprisingly, this method yields ultradisperse diamond (UDD) with a narrow (typically 5 Å) distribution of particle sizes centered around 50 Å [2–12], whereas the alternative way based on detonation compression of graphite leads to the production of diamond particles in the wider nanometer–micrometer range [13].

Most previous studies on the detonation synthesis process have been done at military or commercial plants, and thus only several reports are available for the scientific community. It was shown [2–5] that the increase in pressure during explosion leads to a higher

diamond content in the detonation soot that determined the choice of strong explosives [typically a mixture of trinitrotoluene (TNT) and hexogene] as initial substances. The importance of the way of cooling of the product after the detonation was shown in Refs. [3–6]: an increase in density and heat capacity of the coolant (in a series of gases: vacuum, N₂, Ar, CO₂, and liquid water) led to an increase in the diamond content in detonation soot. The reasons for that have been discussed in Refs. [6,7] on the basis of the diamond–graphite pressure–temperature (*P–T*) phase diagram. After explosion the pressure and temperature in the chamber drop, passing the undesirable *P–T* region where the graphite phase is more stable than diamond and where the temperature is still high enough for diamond–graphite conversion. An increase in the density and heat capacity of coolants led to an increase in the cooling rate and, therefore, a reduction in the residence time in the undesirable *P–T* zone. Nevertheless, in spite of the successful interpretation of the detonation results, care should be taken when determining the content of the detonation product on the basis of the static carbon *P–T* diagram, since it may be not be adequate for a nonequilibrium (with a time scale of about 1 μs [2]) detonation process and does not take into account the formation of amorphous carbon (a-C) phases.

Increasing availability of UDD in the last few years has stimulated research on its physical properties. Direct

* Corresponding author. Fax: +32-16-32-7987.

E-mail address: kostya.iakoubovskii@fys.kuleuven.ac.be (K. Iakoubovskii)

observation of UDD in high-resolution electron microscopy [9,10] showed that UDD particles with a mean size of about 50 Å agglomerate in bigger clusters (up to hundreds of nanometers). Individual particles are mainly of cubic diamond, with some structural defects inside, surrounded by a shell of a non-diamond substance. On the basis of X-ray diffraction (XRD) and small-angle X-ray scattering (SAXRS) measurements [6–8] it was suggested that the structure of this shell depends on the method of cooling and cleaning of the detonation product. A shift in the diamond Raman line [6,11] was observed and interpreted in terms of a quantum confinement effect in small diamond particles. In Ref. [11], on the basis of ultraviolet and X-ray photoelectron spectroscopy (UPS and XPS) results, the Fermi level position in UDD was determined as $E_C - 1.7$ eV; also, the percent concentrations of nitrogen and oxygen atoms in UDD were detected. Infrared (IR) transmission measurements [12] showed that, when exposed to the ambient conditions, UDD readily absorbs atmospheric water. After that the O–H vibrations dominate the IR spectrum, which also contain different C–H and C–O groups. Electron spin resonance (ESR) on UDD powder [14,15] revealed a single band at $g = 2.0028$ with a width of 11 G and spin concentration of about 1000 ppm, which has been attributed to the carbon dangling bond. IR–visible absorption spectra [15] showed only a broad band with a threshold at around 1 eV, typical for a-C. In Ref. [15], on the basis of ESR, transmittance and Raman results, it was suggested that a-C is a dominant defect in UDD. No characterization of UDD by proton nuclear magnetic resonance (^1H NMR) has been reported so far, in contrast with the several ^1H NMR studies of chemical vapor deposited (CVD) diamond that have been reported [16]. All of those studies were performed in static conditions and showed bands, strongly broadened by the dipole–dipole interaction. Rotation of the sample at an angle θ with respect to the direction of the magnetic field, determined from the condition $3 \cos^2(\theta) - 1 = 0$, in magic angle spinning proton NMR (^1H MAS NMR) allows one to suppress this interaction.

In the present work we report a comparative study of the physical properties of nanodiamond, obtained under different synthesis conditions, by means of XRD, ^1H MAS NMR, ESR and IR transmittance.

2. Experimental

Diamond soot was obtained by detonation of 60/40 mixture of TNT/hexogene in a gaseous CO_2 (hereafter called ‘dry synthesis’) or water (‘wet synthesis’) medium [6–8]. UDD was separated using either a continuous flow of nitric acid at temperature of about 250°C [6–8] or ozone treatment (‘ozone UDD’). Ozone cleaning was

performed for the wet synthesis UDD only, in a commercial setup; similar results were obtained for cleaning by ozone generated using a low-pressure Xe lamp equipped with an MgF_2 window.

All measurements, except the NMR, were performed at room temperature under atmospheric pressure. XRD and SAXRS were measured with a ‘Rigaku Cor’ diffractometer operating at 1.541 83 Å. IR transmittance was measured on a thin layer of powder, placed between two ZnS plates. ESR spectra were recorded with a Bruker Q-band (35 GHz) spectrometer. ^1H MAS NMR measurements were performed at room temperature in a magnetic field of 7 T (rf 300 MHz). Since UDD readily absorbs atmospheric water, which strongly affects ^1H MAS NMR measurements, all UDD powders were annealed for overnight at 120°C in vacuum 10^{-2} Torr and then transferred in a dry nitrogen atmosphere to the NMR spectrometer. The reliability of such a method of water removal is supported by the long experience of work with zeolite powders, known as extremely hydrophilic substances. Except for the NMR, measurements were multiply repeated on different batches of the UDD powder from different synthesis runs.

3. Results

Visual examination of the purified powders revealed a strong difference in their color for similar amounts of material with similar morphology. The wet synthesis powder was black, whereas the dry synthesis powder was gray and the ozone-cleaned powder was light gray. Combined XRD and SAXRS spectra are shown in Fig. 1. Peaks at the diffraction angles $2\theta = 43.9^\circ$, 75.3° and 91.5° correspond to diamond (111), (220) and

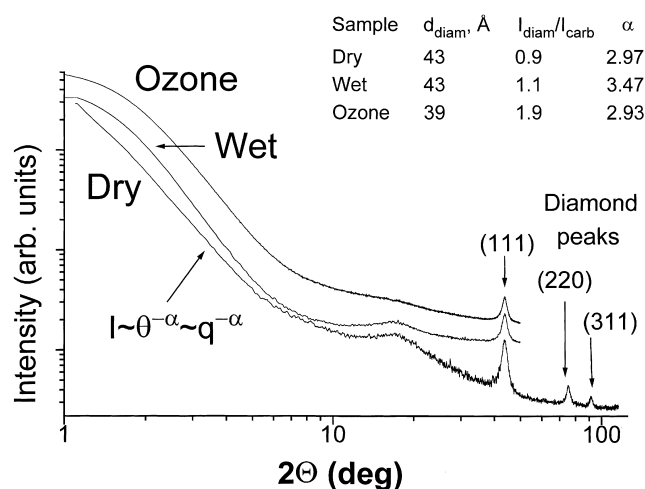


Fig. 1. Combined XRD and SAXRS spectra for the dry, wet and ozone UDD powders. Inset shows the values of the diamond particle diameter d_{diam} , ratio of integrated intensities of the 43.9° to the 17° peaks $I_{\text{diam}}/I_{\text{carb}}$, and exponent α derived from XRD graphs.

(311) reflections. From the width of these peaks the mean diameter of diamond particles d_{diam} was calculated using the Debye formula. This diameter determined from any of the diamond peaks was the same within experimental error ($\pm 5 \text{ \AA}$), demonstrating that the broadening of the diamond peaks is probably due to the small particle size, but not due to the internal stress. The latter would cause different broadening for different peaks. In the small-angle part of Fig. 1 the intensity of the scattered X-ray radiation increases with a decrease in the scattering angle θ as $I \approx \theta^{-\alpha}$. It is more convenient to express θ versus wave vector $q = (4\pi/\lambda) \sin(\theta)$. At small θ , $I \approx \theta^{-\alpha} \approx q^{-\alpha}$. The peak at 17° , which is equivalent to $q_{\text{max}} = 1.2 \text{ \AA}^{-1}$, is attributed to the X-ray scattering on small non-diamond carbon clusters [6–8]. From the maximum position the size of the scattering element in a cluster can be estimated as $d_{\text{scatt}} \cong \pi/q_{\text{max}} = 2.6 \text{ \AA}$, which is very close to the diameter of a carbon hexagon, whereas from the linewidth the mean diameter of the cluster was calculated as 15 \AA . The ratio of integrated intensities of the 43.9° to the 17° peak $I_{\text{diam}}/I_{\text{carb}}$, as well as values of d_{diam} , and α for all powders studied are summarized in the inset in Fig. 1.

IR spectra (not shown) were similar to those published in Ref. [12]. In all samples studied the dominant absorption band was centered at 3400 cm^{-1} with a width of 500 cm^{-1} , accompanied by a sharper peak at 1630 cm^{-1} . These peaks were shown to originate from the O–H vibrations [12]. Also, absorption bands around 2950 , 1750 , 1300 , 1100 cm^{-1} are observed in our spectra and ascribed to different C–H, C=C, C=O and C–O–C groups [17].

^1H MAS NMR spectra, along with their deconvolution to a sum of Gaussian bands, are presented in Fig. 2. According to the NMR standards, absorption lines are plotted versus their shift $\Delta\nu$ from the position of the resonance ν_0 for the reference substance $\text{Si}(\text{CH}_3)_4$. This chemical shift is normalized to the ν_0 and expressed in parts per million (ppm). Positions, widths and integrated amplitudes of the NMR lines are summarized in Table 1. Different amounts of powder were used to record the NMR curves of Fig. 2 and, therefore, no comparison of absolute amplitudes is possible; however, our estimates show that the integrated amplitude of the total NMR signal was the smallest for the wet synthesis powder. The data of Fig. 2 and Table 1 show the strong difference

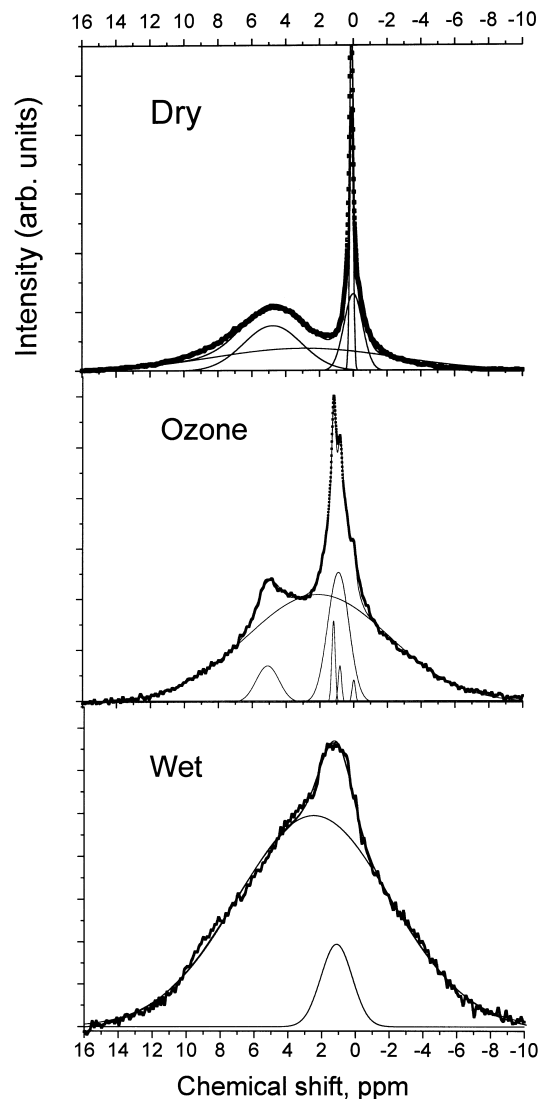


Fig. 2. ^1H MAS NMR spectra for the wet, ozone and dry UDD powders.

in the position and amplitude of the NMR signals for different samples: two bands with a width of about 10 and 1.5 ppm centered around 2.5 ppm and 0.5 ppm are present in all three spectra; however, the narrow line structure around 0 ppm is specific for every sample and is absent for the wet synthesis sample. Dry and ozone powders also show a broad band around 5 ppm, which is also absent for the wet synthesis powder. Remarkable

Table 1
Deconvolution of NMR spectra to Gaussian components^a

Sample	X_c	w	I	X_c	w	I	X_c	w	I	X_c	w	I	X_c	w	I	X_c	w	I
Dry	2.8	10.7	10.4	0.4	1.2	3.6	4.8	3.4	6.6	0.1	0.2	1.1						
Wet	2.5	9.4	11.7	1.1	1.8	0.9												
Ozone	2.2	8.6	11.3	0.9	1.3	2	5	1.3	0.6	0	0.2	0.06	0.8	0.2	0.09	1.2	0.2	0.2

^a X_c (ppm) and w (ppm) are the position and linewidth respectively; I (arb. units) is the integrated intensity.

is the difference in the relative contribution of the broadest band to the NMR spectrum for the dry and wet synthesis (after either ozone- or acid-cleaning) powders, which should be ascribed to the difference in the synthesis conditions. Interpretation of the individual bands is complicated, because different chemical groups can give rise to NMR lines in the considered range of chemical shifts. On the basis of our IR results and known values for the chemical shifts from the certain chemical groups [18], we suggest the following interpretation of the NMR spectra of Fig. 2. The sharp peaks around 0 ppm in dry and ozone powders and broad bands at 2.5 and 0.5 ppm may be ascribed to CH, CH₃ and CH₂ groups in different configurations. The broadness of the 2.5 and 0.5 ppm bands is due to an overlap of several peaks with the central positions mutually shifted due to the different configuration at the carbon site, e.g. C=CH₂, C-CH₂, O=CH₂, O-CH₂, N-CH₂, etc. The relative sharpness of the peaks around 0 ppm in the dry and ozone powders suggests that they are due to some groups in a certain fixed configuration, in our opinion being C-CH₂ and C-CH₃. The band at 5 ppm in the same samples we assign to the -OH group.

ESR spectra (not shown) revealed a single band at $g=2.003$. The determined linewidth and concentrations of spins were 9.6 G, 1100 ppm and 8.8 G, 1300 ppm for the wet and dry synthesis samples respectively. As for NMR, the ESR resonance line is broader for the wet synthesis than for the dry synthesis powder; however, the similarity in concentration of paramagnetic centers suggests that neither spin-spin nor spin-nuclear interaction can be responsible for the difference in the linewidth.

4. Discussion

The theory of SAXRS states that, in the range of the wave vectors q where the intensity of SAXRS obeys the law $I \approx q^{-\alpha}$, $\alpha=3$ for a bulk and $\alpha=4$ for a surface material [19]. The values of α (see inset in Fig. 1) are close to 3 for the dry and ozone samples, in accordance with the theory, whereas the wet synthesis UDD shows the α value close to 3.5. Two reasons for the deviation from $\alpha=3$ and 4 are known [19]: a large dispersion in the mean diameter of the scattering objects and a different, possibly fractal-like [6–8], surface roughness. XRD data show that in our case the scattering objects are diamond grains, with a narrow distribution of the mean diameter, surrounded by a non-diamond shell. Therefore, the deviation from $\alpha=3$ in the wet synthesis powder and the difference in α for different powders can be explained by the peculiarities in the composition of the UDD shell, having either a large dispersion in thickness or fractal-like structure. The NMR spectra of

Fig. 2 provide confirmation for the proposed difference. The NMR curves for the dry and ozone powders show similar well-defined lines, and similar values of α were obtained (see inset in Fig. 1), whereas the NMR curve, as well as the value of α , is distinctly different for the wet synthesis UDD.

The black color of the wet synthesis powder, much darker than the color of the dry synthesis UDD, suggests a higher content of the graphite-like carbon in the former material. XRD spectra of Fig. 1 show no presence of graphite in any powder studied. A peak at 17°, attributed to small graphite-like clusters, is seen for all samples; however, the strength of this band is comparable in the dry and wet synthesis UDD. It is known that the band gap of the a-C strongly depends on its microscopic structure [20]. The difference in the color of the dry and wet synthesis powders may be explained by the suggested above difference in the structure of the a-C shell, surrounding the diamond particles: the shell of the wet synthesis UDD possibly contains a-C with a band gap that is narrower than in the dry synthesis UDD, leading to the darker coloration.

ESR results show that although UDD was produced from a mixture containing comparable concentrations of carbon and nitrogen atoms, no nitrogen-related center was detected. Although it is hypothetically possible to have all nitrogen atoms in diamond in diamagnetic form, e.g. as neutral di-nitrogen centers, ESR measurements on natural diamond [21] show that, in practice, a considerable part of them is charged and, therefore, ESR-active. Moreover, the short duration of the detonation process suggests that if nitrogen atoms incorporate into UDD grains they should be mostly present as single substitutional (the so-called P1) centers. The results of Ref. [11] suggest a Fermi level position in UDD close to the energy position of the P1 center, $E_C - 1.7$ eV [21]; therefore, a significant part of P1 centers should be in the occupied, paramagnetic state. The absence (<10 ppb) of the P1 ESR signal in UDD suggests that nitrogen atoms do not incorporate into the UDD grains. They possibly remain in the UDD shell or in non-diamond structures, which are removed during the purification procedure.

5. Summary and conclusions

The characterization of the structure and defects in detonation synthesis diamond is reported. XRD and NMR results are interpreted in terms of the different structure of the diamond particles, produced at different conditions. In spite of the comparable contents of carbon and nitrogen in the precursor, no paramagnetic nitrogen was detected in the diamond grains.

Acknowledgement

The authors are indebted to the NATO linkage grant HT 97 3290 for financial support.

References

- [1] S. Veprek, *Thin Solid Films* 297 (1997) 145.
- [2] N.R. Greiner, D.S. Phillips, J.D. Johnson, F. Volk, *Nature* 333 (1988) 440 and references cited therein.
- [3] V.M. Titov, V.F. Anisichkin, I.Yu. Mal'kov, *Fizika Goreniya i Vzryva* 25 (1989) 117.
- [4] A.I. Lyamkin, E.A. Petrov, A.P. Ershov, G.V. Sakovich, A.M. Staver, *Sov. Phys. Dokl.* 33 (1988) 705.
- [5] E.A. Petrov, G.V. Sakovich, P.M. Brylyakov, A.P. Ershov, *Sov. Phys. Dokl.* 35 (1990) 765.
- [6] A.E. Alexensky, M.V. Baidakova, A.Ya. Vul', V.Yu. Davydov, Yu.A. Pevtsova, *Phys. Solid State* 39 (1997) 1007.
- [7] M.V. Baidakova, A.Ya. Vul', V.I. Siklitskii, N.N. Faleev, *Phys. Solid State* 40 (1998) 715.
- [8] A.E. Aleksenskii, M.V. Baidakova, A.Ya. Vul', V.I. Siklitskii, *Phys. Solid State* 41 (1999) 668.
- [9] L.A. Bursill, J.L. Peng, S. Praver, *Philos. Mag. A*: 76 (1997) 769.
- [10] E.D. Obratsova, M. Fujii, S. Hayashi, V.L. Kuznetsov, Yu.V. Butenko, A.L. Chuvilin, *Carbon* 36 (1998) 821.
- [11] E. Maillard-Schaller, O.M. Kuettel, L. Diederich, L. Schlapbach, V.V. Zhirnov, P.I. Belobrov, *Diam. Relat. Mater.* 8 (1999) 805.
- [12] Sh. Ji, T. Jiang, K. Xu, Sh. Li, *Appl. Surf. Sci.* 133 (1998) 231.
- [13] D.G. Morris, *J. Appl. Phys.* 51 (1980) 2059.
- [14] L.G. Karaseva, T.A. Karpukhina, B.V. Spitsyn, *Russ. J. Phys. Chem.* 57 (1983) 724.
- [15] K. Iakoubovskii, G.J. Adriaenssens, K. Meykens, M. Nesládek, A.Ya. Vul', V.Yu. Osipov, *Diam. Relat. Mater.* 8–9 (1999) 1476.
- [16] M. Pruski, D.P. Lang, S.-J. Hwang, H. Jia, J. Shinar, *Phys. Rev. B* 49 (1994) 10 635.
- [17] W.W. Simons (Ed.), *The Sadtler Handbook of Infrared Spectra*, Sadtler Research Laboratories, 1978.
- [18] H. Gunther, *NMR Spectroscopy*, Wiley, 1980.
- [19] P. Wong, *Phys. Rev. B* 32 (1985) 7417.
- [20] J. Robertson, *Adv. Phys.* 35 (1986) 317.
- [21] J.H.N. Loubser, J.A. van Wyk, *Rep. Prog. Phys.* 41 (1978) 1201.